



DIPLOMA THESIS

CFD ANALYSIS OF FLOW IN A FISH TANK

**DEPARTMENT OF PROCESS ENGINEERING
CZECH TECHNICAL UNIVERSITY IN PRAGUE**

2019

MURAT IPEK



MASTER'S THESIS ASSIGNMENT

I. Personal and study details

Student's name:	Ipek Murat	Personal ID number:	472154
Faculty / Institute:	Faculty of Mechanical Engineering		
Department / Institute:	Department of Process Engineering		
Study program:	Mechanical Engineering		
Branch of study:	Process Engineering		

II. Master's thesis details

Master's thesis title in English:
CFD analysis of flow in a fish tank

Master's thesis title in Czech:
CFD analýza toku v nádrži pro chov ryb

Guidelines:

- Make a basic literature review concerning the flow configurations in fish tanks.
- Make a grid independence study for the given geometry.
- Compare several turbulence models and choose a suitable model for the consequent simulations.
- Perform numerical simulations and compare the results with available experimental data.
- Summarize the methodology used in the thesis and propose possible improvements of the solution procedure.

Bibliography / sources:
According to the recommendation of the supervisor.

Name and workplace of master's thesis supervisor:
doc. Ing. Karel Petera, Ph.D., Department of Process Engineering, FME

Name and workplace of second master's thesis supervisor or consultant:

Date of master's thesis assignment: **23.04.2019** Deadline for master's thesis submission: **07.06.2019**

Assignment valid until: _____

 _____ doc. Ing. Karel Petera, Ph.D. Supervisor's signature	 _____ prof. Ing. Tomáš Jirout, Ph.D. Head of department's signature	 _____ prof. Ing. Michael Valášek, DrSc. Dean's signature
--	---	--

III. Assignment receipt

The student acknowledges that the master's thesis is an individual work. The student must produce his thesis without the assistance of others, with the exception of provided consultations. Within the master's thesis, the author must state the names of consultants and include a list of references.

<u>30-04-2019</u> Date of assignment receipt	 _____ Student's signature
---	----------------------------------

Annotation sheet

Name: Murat

Surname: Ipek

Title in Czech: CFD analýza toku v nádrži pro chov ryb

Title in English: CFD analysis of flow in a fish tank

Scope of work: number of pages: 52

number of figures: 22

number of tables: 12

number of appendices: 1

Academic year: 2018/2019

Language: English

Department: Process Engineering

Specialization: Process Engineering

Supervisor: doc. Ing. Petera Karel Ph.D.

Reviewer:

Submitter: Czech Technical University in Prague. Faculty of Mechanical Engineering,
Department of Process Engineering

Annotation - Czech:

Annotation – English: Make literature research concerning the flow configurations in fish tanks. Make a grid independence study for the given geometry. Compare several turbulence models and choose a suitable model for the consequent simulations. Perform numerical simulations and compare the results with available experimental data. Summarize the methodology used in the thesis and propose possible improvements of the solution procedure.

Keywords: Fish tank, CFD, ANSYS, turbulence intensity, average velocity, uniformity index, maximum velocity, k- ϵ turbulence model.

Utilization: For Department of Process Engineering, Czech Technical University in Prague.

Declaration

I hereby declare that I have completed this thesis entitled **CFD analysis of flow in a fish tank** independently with consultations with my supervisor and I have attached a full list of used references and citations.

I do not have a compelling reason against the use of the thesis within the meaning of Section 60 of the Act No. 121/2000 Coll., on copyright, rights related to copyright and amending some laws (Copyright Act).

In Prague, 06.08.2019

Murat Ipek
Signature

ACKNOWLEDGEMENT

I hereby wish to express my appreciation and gratitude to the supervisor of my thesis, Doc. Ing. Karel Petera, Ph.D. for his unfailing support, advice, and guidance.

I also would like to express my gratitude to Ing. Stepan Papacek, Ph.D. for valuable advice and comments during my work.

ABSTRACT

A CFD analysis of flow in a fish tank was performed in ANSYS Fluent using the realizable $k-\epsilon$ model with enhanced wall treatment. A grid independence study which was based on the average velocity showed discretization error. Average velocities, turbulence intensity, and maximum velocity were calculated with ANSYS Fluent and described by a single correlation for three sizes of tanks. Such correlation could be used by biologist when designing a fish tank of a given volume and choosing proper operational parameters. Additionally, uniformity index was calculated for three sizes of tanks.

Keywords: Fish tank, CFD, ANSYS, turbulence intensity, average velocity, uniformity index, maximum velocity, $k-\epsilon$ turbulence model.

Table of Contents

List of Figures	7
List of Tables.....	7
List Of Symbols	8
1. Introduction	9
1.1. Computational Fluid Dynamics	10
1.1.1. Process of CFD	11
1.1.2. Governing Equations	11
1.2. Turbulent Flow	13
1.2.1. Turbulence Modelling.....	15
1.2.2. Direct Numerical Simulation (DNS).....	15
1.2.3. Large Eddy Simulation (LES).....	15
1.2.4. Reynolds Averaged Navier-Stokes (RANS)	16
1.2.5. Turbulent Boundary Layer	18
2. Objectives and Motivation	20
3. Model Description and Methodology.....	21
3.1. Geometry and Mesh Description.....	21
3.2. Grid Convergence Index.....	25
3.3. Solver Settings	28
3.4. Symmetry	32
3.5. Bigger and Smaller Size Geometry Description	34
4. Results	35
5. Conclusion.....	46
REFERENCES	48
Appendix A	49

List of Figures

Figure 1	Process of Computational Fluid Dynamics (Zuo,2005)	11
Figure 2	Classification of flow(Aerospace, Mechanical & Mechatronic Engg. University of Sydney, 2005)	14
Figure 3	Typical point velocity measurement in a turbulent flow (Ansys Training Material,2014)	16
Figure 4	Dimensionless boundary layer profile (ANSYS Training Material 2014)	19
Figure 5	Tank drawings and dimensions of the three tanks of volumes (a)40, (b)500 and (c)2000 liters(Lika et al.,2015)	22
Figure 6	Obtained Geometry	23
Figure 7	50 mm global size mesh	24
Figure 8	23 mm global size mesh	25
Figure 9	Monitored quantity to mesh size	25
Figure 10	Average velocity vs size of the element	27
Figure 11	Bottom medium and surface planes in 545L tank.	30
Figure 12	The k- ω SST intermitting transitional model	32
Figure 13	The Spalart Allmaras model	33
Figure 14	Realizable k- ϵ with enhanced wall treatment	34
Figure 15	Created planes view after scaling	35
Figure 16	u_{avg} vs \dot{V}/V	38
Figure-17	u_{avg}^* vs \dot{V}/V	39
Figure 18	Max(u_{avg}) vs Volume	40
Figure 19	$u_{ref} = \max(u_{avg})$	41
Figure-20	u_{max}^* vs \dot{V}/V	43
Figure 21	Turbulence Intensity vs \dot{V}/V	44
Figure 22	Uniformity Index of three sizes of tanks	45

List of Tables

Table 1	Quality of Meshes	23
Table 2	GCI results in different turbulence model with 845000 mesh	27
Table 3	Experimental results with velocities at different planes with \pm values(Lika.K et al. 2015)	28
Table 4	Velocities of each point	29
Table 5	Experimental average velocities	30
Table 6	Calculated average velocities with errors	30
Table 7	Vertical distances of planes in figure 15	35
Table 8	Calculated turbulent intensity, uniformity index, average, and maximum velocity	37
Table 9	Corresponding values for average velocity	42
Table 10	Corresponding values of u_{max}^*	43
Table 11	Corresponding values of $turb_{max}^*$	44
Table 12	Uniformity index for three sizes of tanks	45

List Of Symbols

ρ	Fluid density	kg/m ³
∇	Nabla operator	
u, \vec{u}	Instantaneous Velocity	m/s
∇p	Gradient of pressure	Pa
t	time	s
p	Static pressure	Pa
$\bar{\tau}$	Viscous stress tensor	Pa
τ_{wall}	Wall Shear stress	Pa
g	Gravitational force	m/s ²
F	Outer forces	-
Re	Reynolds number	-
\bar{u}, U	Mean velocity	m/s
u'	Fluctuating velocity	m/s
L	Characteristic Length	m
μ	Dynamic viscosity	Pa.s
μ_t	Turbulent viscosity	m ² /s
k	Kinetic turbulence energy	J
ε	Dissipation rate	m ² /s ³
ω	Dissipation rate	m ² /s ³
C_μ	k- ε model's constant	-
u^+	Dimensionless velocity	-
Y	Distance from the wall	m
Y^+	Dimensionless distance	-
u_{avg}	Area-Weighted average velocity	m/s
u_{avg}^*	Dimensionless velocity	-
u_{ref}	Reference velocity	m/s
\dot{V}	Volumetric flow rate	m ³ /s

1. Introduction

Nowadays, the food industry is overgrowing in order to meet the emerging demand for food due to the increasing amount of people. This demand includes all areas of food products, but it can be said that seafood has a significant proportion. Since consumers have become aware of the positive effect on the health of eating fish, they tend to consume more rather than eating chicken, beef, or pork.

Nevertheless, there are some limitations for natural fisheries in producing seafood such as the prohibition of catching fishes in some period. On the other hand, the uncertainty of the daily amount caught fishes creates a barrier for natural fisheries. Thus, it creates a demand for aquaculture tanks in order to provide the necessary support in the marketplace and meet the demand of consumers.

Besides these, fish tanks have an impact on the economies since it creates new job opportunities for thousands of people in many countries.

According to the Environmental Defense Fund, a non-profit environmental organization, global fisheries exports now earn more revenue than any other traded food commodity in the world, including rice, cocoa, or coffee (Souza,2018).

With the emerging fisheries industry, the amount of the problems which were faced started to increase. On the other hand, the most significant challenge is the cleaning and sedimentation problem of tanks.

In this study, the main scope was to find the best CFD model for fish tanks. Focus is mainly put on how to choose operating parameters giving good living conditions in fish tanks. When choosing the operation parameters, we tried to find the best turbulence model, which would correctly describe the given system.

Besides focusing on operating parameters, the secondary aim of the study was to find suitable design parameters. In the industry, mostly rectangular tanks are preferred, and this creates a big problem regarding cleaning due to the dead zones in the tanks where there is no flow. Hence, the methodology described in this thesis can be used to determine proper parameters and geometry configuration with respect to self-cleaning characteristics.

In order to reach these objectives, ANSYS Fluent software is used, and the model obtained. After this, it is compared with some experimental data.

In the CFD model of the study, the first focus was flow pattern as it is crucial for fish tanks for some reasons which are explained below:

- For the fish itself: Generally, uniform velocities are preferred in fish tanks without high peaks. Sometimes zones with small velocities where the fishes can have a rest are necessary.
- For self-cleaning: Particles such as feed pellets or excrements should not stay for a long time in the tank, and it would be nice if they naturally left the tank through the outlet.

1.1. Computational Fluid Dynamics

Computational fluid dynamics (CFD) is a science that produces quantitative predictions of fluid-flow phenomena based on the conservation laws (conservation of mass, momentum, and energy) governing fluid motion with the help of digital computers (Howard, 2012).

At present, fluid mechanical problems are more significant than the previous time because technology is rapidly improving and going to be more complicated in the future. Because of that, the analytical solution of these models became almost impossible these days. This reason provided CFD is the most popular software recently because people demand an easier way to find a solution for Fluid Mechanics. On the other hand, the software has a user-friendly interface, and it can be used for many aims which can be seen below. Some examples can be given as:

- Aerodynamics of aircraft and vehicles
- Turbomachinery
- Optimizing
- Chemical process engineering
- Hydrology and Oceanography

1.1.1. Process of CFD

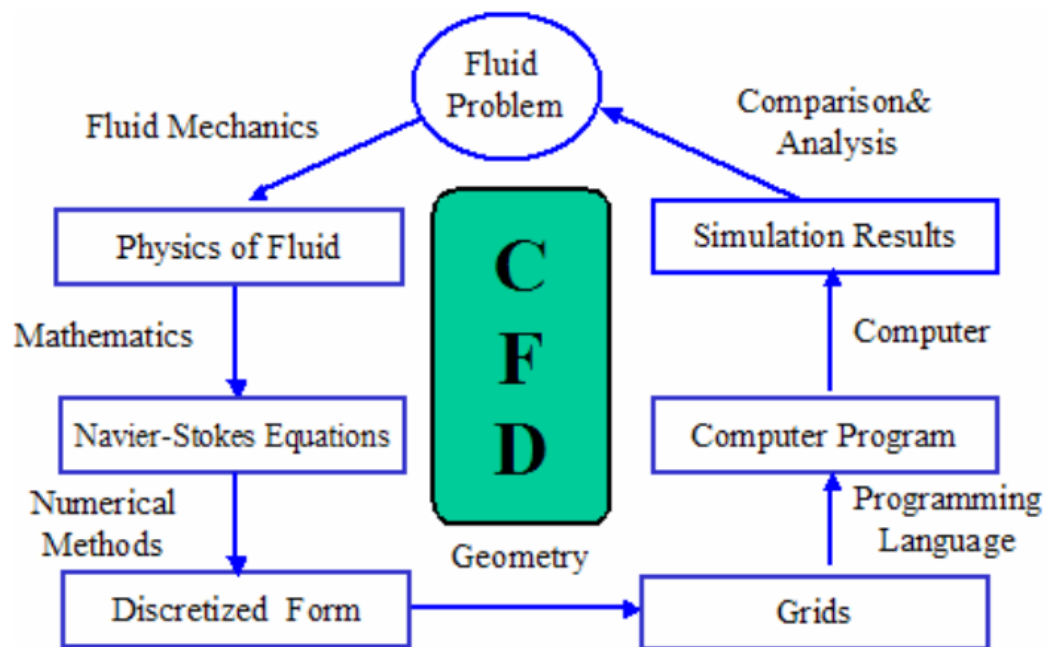


Figure 1 Process of Computational Fluid Dynamics (Zuo,2005)

First of all, there is a fluid problem which can be described by using Fluid Mechanics. After that, some mathematical equations can be used to describe the flow field in a given problem. It can be said the best equation of this case is the Navier-Stokes Equation. It can give us an analytical solution for very simple cases. However, as mentioned above, problems are getting complicated. Hence, a computer is needed to solve equations. When a computer is used, the problem is transformed to the discretized form by finite difference, finite element, or finite volume methods.

1.1.2. Governing Equations

Regarding CFD, main equations based on the conservation of fundamental physical properties like mass and momentum are described below.

1.1.2.1. Conservation of Mass

The continuity equation can be expressed by the mass balance of a system (control volume). For compressible fluids (fluids with changeable density), it is described as:

$$\frac{\partial \rho}{\partial t} + \nabla \cdot (\rho \vec{u}) = 0 \quad (1)$$

The first term represents the rate of change of the density in time — the second term represents the net flow of mass through boundaries. For incompressible fluid (fluid with constant density) the equation (1) becomes:

$$\nabla \cdot \vec{u} = 0 \quad (2)$$

1.1.2.2. Conservation of Momentum

The ratio of momentum change to time is equal to the resultant force affecting continuity and is obtained by Cauchy momentum equation; it is applied for solids and liquids.

$$\rho \left(\frac{\partial \vec{u}}{\partial t} + \vec{u} \cdot \nabla \vec{u} \right) = -\nabla p + \nabla \cdot \vec{\tau} + \rho g + F \quad (3)$$

Here, p stands for static pressure, and $\vec{\tau}$ is viscous stress tensor, ρg is the gravitational forces and F stands for the outer forces.

The Navier-Stokes equation is a particular case of Cauchy's equation. It is applied for incompressible Newtonians fluids (constant density):

$$\rho \left(\frac{\partial \vec{u}}{\partial t} + \vec{u} \cdot \nabla \vec{u} \right) = -\nabla p + \mu \nabla^2 \vec{u} + \rho g \quad (4)$$

\vec{u} stands for the velocity, ∇p represents the gradient of pressure, μ is the dynamic viscosity, ρ implies density and g is the gravity force.

It is not possible to solve these equations analytically for most of the engineering problems. However, it is possible to obtain an approximate computer-based solution to the governing equations for a variety of engineering problems (Bhaskaran and Collins, 2012).

1.1.2.3. Finite Volume Method

The Finite Volume Method (FVM) is a numerical technique that transforms the partial differential equations representing conservation laws into discrete algebraic equations over finite volumes (or elements or cells) (Moukalled et al.,2015).

In a similar manner to the finite difference or finite element method, the first step in the solution process is the discretization of the geometric domain, which, in the FVM, is discretized into non-overlapping elements or finite volumes. The partial differential equations are then discretized or transformed into algebraic equations by integrating them over each discrete element. The system of algebraic equations is then solved to compute the values of the dependent variable for each of the elements. These characteristics have made the Finite Volume Method quite suitable for the numerical simulation of a variety of applications involving fluid flow, heat and mass transfer. From a limited potential at inception confined to solving simple physics and geometry over structured grids, the FVM is now capable of dealing with all kinds of complex physics and applications (Moukalled et al.,2015)

1.2. Turbulent Flow

Turbulence is the irregularity of a liquid or gas in motion. Turbulent flow generally occurs at higher flow rates and with larger pipes. Reynolds numbers (Re) define (non-dimensional) whether flow conditions cause laminar or turbulent flow;

$$Re = \frac{\bar{u}L\rho}{\mu} \quad (5)$$

While \bar{u} represents mean velocity, L can be explained as the characteristic length, ρ is density and μ stands for the dynamic viscosity.

According to Reynold number, classification of flows in pipes can be seen below:

$Re < 2300 \rightarrow$ Laminar Flow

$2300 < Re < 4000 \rightarrow$ Transitional Flow.

$Re > 4000 \rightarrow$ Turbulence Flow

A flow can be Laminar, Turbulent or Transitional in nature. This becomes a very important classification of flows and is brought out vividly by the experiment conducted by Osborne Reynolds (1842 - 1912) (Aerospace, Mechanical & Mechatronic Engg. University of Sydney, 2005) We can see the experiment result in the below:

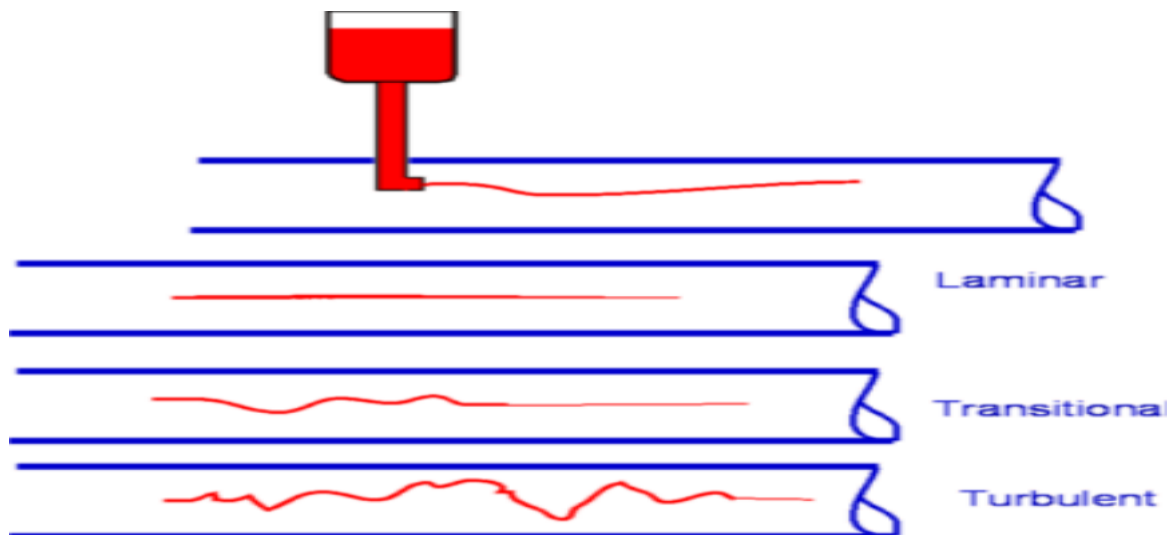


Figure 2 Classification of flow(Aerospace, Mechanical & Mechatronic Engg. University of Sydney , 2005)

1.2.1. Turbulence Modelling

In the CFD simulations, turbulence modeling is generally needed as most of the real engineering cases consist of turbulent flow. On the other hand, there is no universal turbulent model for all engineering applications. The choice of the ideal turbulent model is crucial, in order to provide proper recovery and work safety, and it depends on flow character.

There are three basic approaches to model turbulence;

- Direct Numerical Simulation – DNS
- Large Eddy Simulation – LES
- Reynolds Averaged Navier-Stokes – RANS.

1.2.2. Direct Numerical Simulation (DNS)

In theory, when Navier-Stokes equations can be numerically solved, turbulent flows can be simulated. However, to reach a good result with this method, the mesh must be really fine and time step should be very small. If the Reynolds number is increasing the size of the element needs to decrease in order to able to resolve the smallest scales of turbulent flow. DNS is not the preferred method in complicated cases because it needs a super equipped computer and high technology to solve DNS with fully developed turbulent flow. Nowadays, it is used for fundamentally small systems for the research purposes with low Reynolds number.

1.2.3. Large Eddy Simulation (LES)

The LES method based on modeling large vortexes(eddies) and large-scale turbulent fluctuations can be calculated while small scale eddies are modeled. The mesh can be bigger, and time steps can be larger than DNS. LES method is cheaper than DNS in terms of the computational power required. Hence, LES method is preferred instead of DNS generally, and with advantages of this method, it is possible to obtain a more accurate solution. But still, relatively large computational power is needed with this method.

1.2.4. Reynolds Averaged Navier-Stokes (RANS)

The RANS methods are commonly used in engineering applications. They can be used for a complicated turbulent system when LES and DNS is not able to solve the system due to their large computational requirements.

In general, turbulence is characterized by fluctuations of time-averaged variables (e.g. velocity, pressure, temperature). In figure 3, it can be seen the typical point velocity measurement.

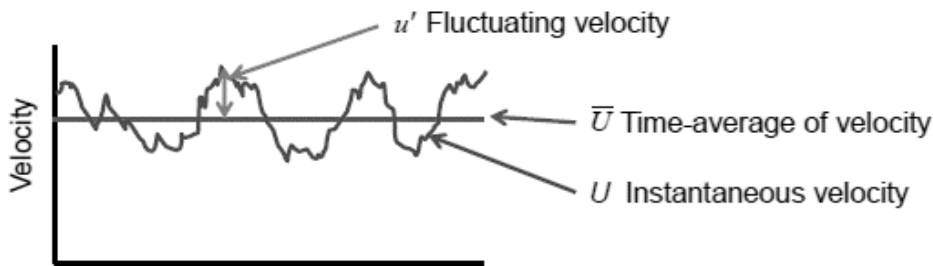


Figure 3 Typical point velocity measurement in a turbulent flow (Ansys Training Material, 2014)

Therefore, it can be described as:

$$u = \bar{u} + u' \quad (6)$$

where \bar{u} is the mean velocity and u' stands for the fluctuating velocity.

If substituting Equation 6 into the Navier –Stokes equation, it can be obtained the RANS equation for mean velocity:

$$\rho \left(\frac{\partial \bar{u}_i}{\partial t} + \bar{u}_k \frac{\partial \bar{u}_i}{\partial x_k} \right) = - \frac{\partial \bar{p}}{\partial x_i} + \frac{\partial}{\partial x_j} \left(\mu \frac{\partial \bar{u}_i}{\partial x_j} \right) + \frac{\partial R_{ij}}{\partial x_j} \quad (7)$$

R_{ij} is the Reynolds stress tensor, which must be described by a turbulence model. There are two types of RANS model:

Reynolds Stress Models (RSM) is a more complex model because it is needed to resolve many other transport equations for all components of the Reynolds stress tensor R_{ij} .

Eddy Viscosity Models assume the stress is comparative to the strain which is the gradients of velocity. Based on the Boussinesq approximation of the turbulent (eddy) viscosity (Hinze, 1975), Reynolds stress tensor is defined as follows:

$$R_{ij} = -\overline{\rho u_i' u_j'} = \mu_t \frac{\partial \bar{u}_i}{\partial x_j} + \frac{\partial \bar{u}_j}{\partial x_i} - \frac{2}{3} \mu_t \frac{\partial \bar{u}_k}{\partial x_k} \delta_{ij} - \frac{2}{3} \rho k \delta_{ij} \quad (8)$$

μ_t is the so called turbulent viscosity. Turbulent viscosity can be expressed as:

$$\mu_t = \rho C_\mu \frac{k^2}{\varepsilon} \quad (9)$$

where C_μ is an empirical constant, k is the turbulent kinetic energy and ε is the dissipation rate of the kinetic energy.

There are many types of RANS turbulence models, three of them are mention below.

Spalart Allmaras model:

It solves the transport equation for the modified viscosity-like variable.

$$\mu_t = f(\tilde{\nu}) \quad (10)$$

where $\tilde{\nu}$ is calling viscosity-like variable.

k-ε model:

It solves the transport equations for k and ε . The related formula is:

$$\mu_t = f\left(\frac{\rho k^2}{\varepsilon}\right) \quad (11)$$

k is turbulent kinetic energy, ε is turbulence dissipation rate

There are three types of k-ε model in ANSYS Fluent:

- Standard k-ε (SKE) model
- Renormalization group (RNG) k-ε model
- Realizable k-ε (RKE) model- this is the recommended variant of k-ε models.

k- ω model:

Solving the transport equations for k and ω . Related formula is:

$$\mu_t = f \left(\frac{\rho k}{\omega} \right) \quad (12)$$

k is turbulent kinetic energy, and ω is a specific dissipation rate

There are two types of k- ω model:

- Standard k- ω (SKW) model
- Shear Stress Transport k- ω (SSTKW) model

1.2.5. Turbulent Boundary Layer

Measurements show that, for both internal and external flows, the streamwise velocity in the flow near the wall varies logarithmically with distance from the surface. This behavior is known as the law of the wall (Wilcox, 2006).

The most essential turbulent boundary layer is the viscous sublayer. It locates slightly further from the wall, and it is bordering with the wall and the log-layer.

The velocity changes quickly close the wall. Generally, using dimensionless velocity shown as:

$$u^+ = \frac{u}{u_t}; u_t = \sqrt{\frac{\tau_{wall}}{\rho}} \quad (13)$$

the velocity of the flow is represented by u , τ_{wall} the wall shear stress and ρ the density of the fluid, and for the dimensionless distance from the wall equation is:

$$Y^+ = \frac{Y u_t}{u} \quad (14)$$

where Y is the distance from the wall. Figure 4 shows an example of the dimensionless boundary velocity profile in a logarithmic scale.

When there is an increase at Reynolds numbers, the logarithmic region will increase to higher values of Y^+ .

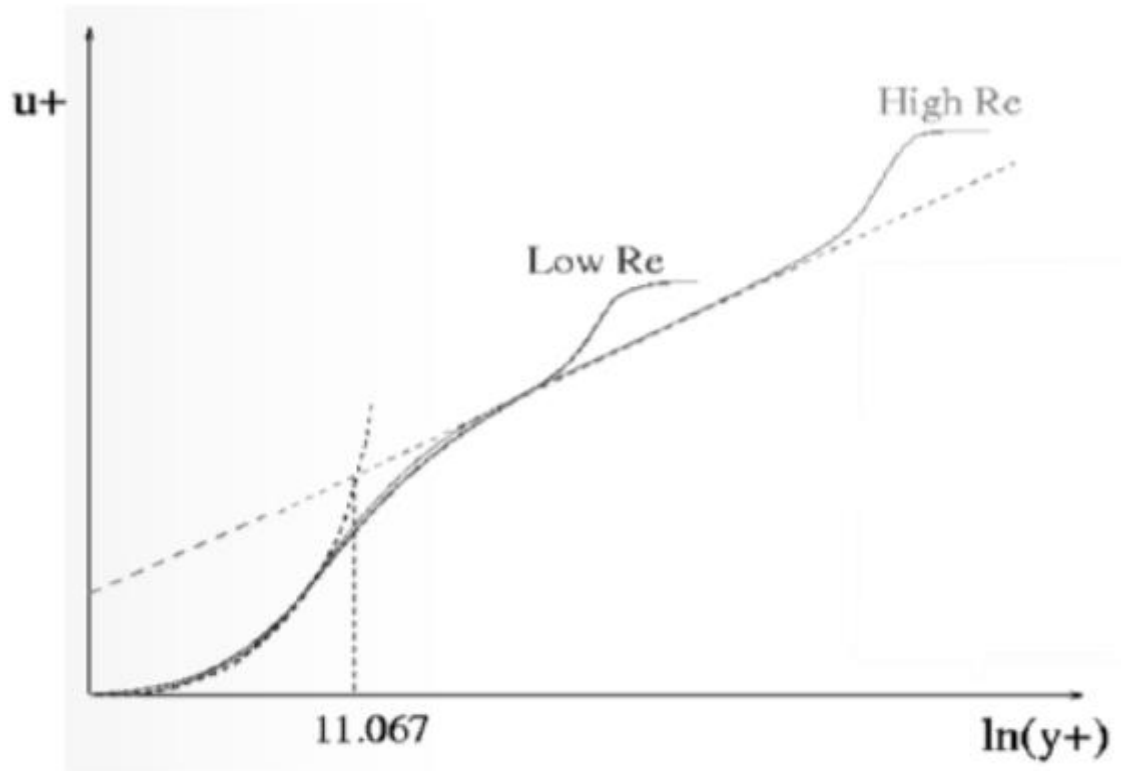


Figure 4 Dimensionless boundary layer profile (ANSYS Training Material 2014)

In the near-wall region, the solution gradients are very high, but accurate calculations in this region are very important for the success of the simulation. There are two approaches:

Wall Functions

This is an approach which is generally used in order to approximate gradients near the wall while the centroid of the adjacent mesh locates in the log-layer and it applies the predictable dimensionless boundary layer. The value of Y^+ should be in between 30 and 300. When the value of the Y^+ is lower than 30, this approach cannot be thought as proper.

From the engineering point of view, this approach provides good results only when the flow is aligned with the wall. Besides this, it is commonly used when mixing in the domain is more important than the forces on the wall.

Resolving The Whole Viscous Sublayer

This approach creates the opportunity to describe the whole viscous sublayer in a proper way. On the other hand, the value of Y^+ should be closer to 1. In this case, the mesh will be adequate in order to resolve the gradients in the sublayer.

Generally, this approach is preferred when the heat transfer is essential for the simulation and it is recommended for the turbulent model commonly for the cases which are SST $k-\omega$ (ANSYS Training Material, 2014).

2. Objectives and Motivation

In the first chapter, the author mentioned the problems which are the increase in human population and eventually increase in demands for the food. Generally, from the environment point of view, people are using incorrect methods to meet the demand such as explosion - based fishing. Thus, they harm the environment, and it creates the same negative effect on the seafood as well. Even though there are many restrictions and explosions which are in use with the purpose of saving the environment, this type of fishing still continues. The motivation of the thesis is to contribute to the fishing industry and to increase fish farming and at the same time to decrease the rate of harmful activities on nature which are done by people.

In this study, firstly parameters are calculated in the Spalart-Allmaras turbulent model. Then, the grid convergence index was analyzed. After that, $k-\epsilon$ and $k-\omega$ turbulent models were used and the symmetricity of results was investigated. To select the most suitable model, all results were compared with the experimental data. The experiment was performed by Lika et al. (2015). In their experiment, larvae were used instead of mature fish therefore the flow conditions like maximum or average velocities might be more important in such case.

3. Model Description and Methodology

The 3-D geometry of the corresponding fish tank (Lika et al., 2015) was created in ANSYS DesignModeler. Then, a tetrahedral mesh was created in ANSYS Meshing, which was later transformed to polyhedral mesh to improve the mesh quality and get better convergence of the solution. Then, ANSYS Fluent solver was used to get results for given boundary conditions (flow rates and inlet velocities were based on data provided by Lika et al., 2015).

3.1. Geometry and Mesh Description

In the experiment (Lika et al., 2015), three different size tanks were used which are shown in Figure 5:

These are 40, 500, and 2000 liters. In this study, 500 liters was used as the initial case. Besides that, according to the experiment, the water circulation rate was $5\% \text{ h}^{-1}$ at the beginning and then it increased to $50\% \text{ h}^{-1}$ (Lika et al., 2015). After this, flowrate and inlet velocity were calculated and obtained as $0.25 \text{ m}^3/\text{hr}$ flow rate and 0.35 m/s velocity.

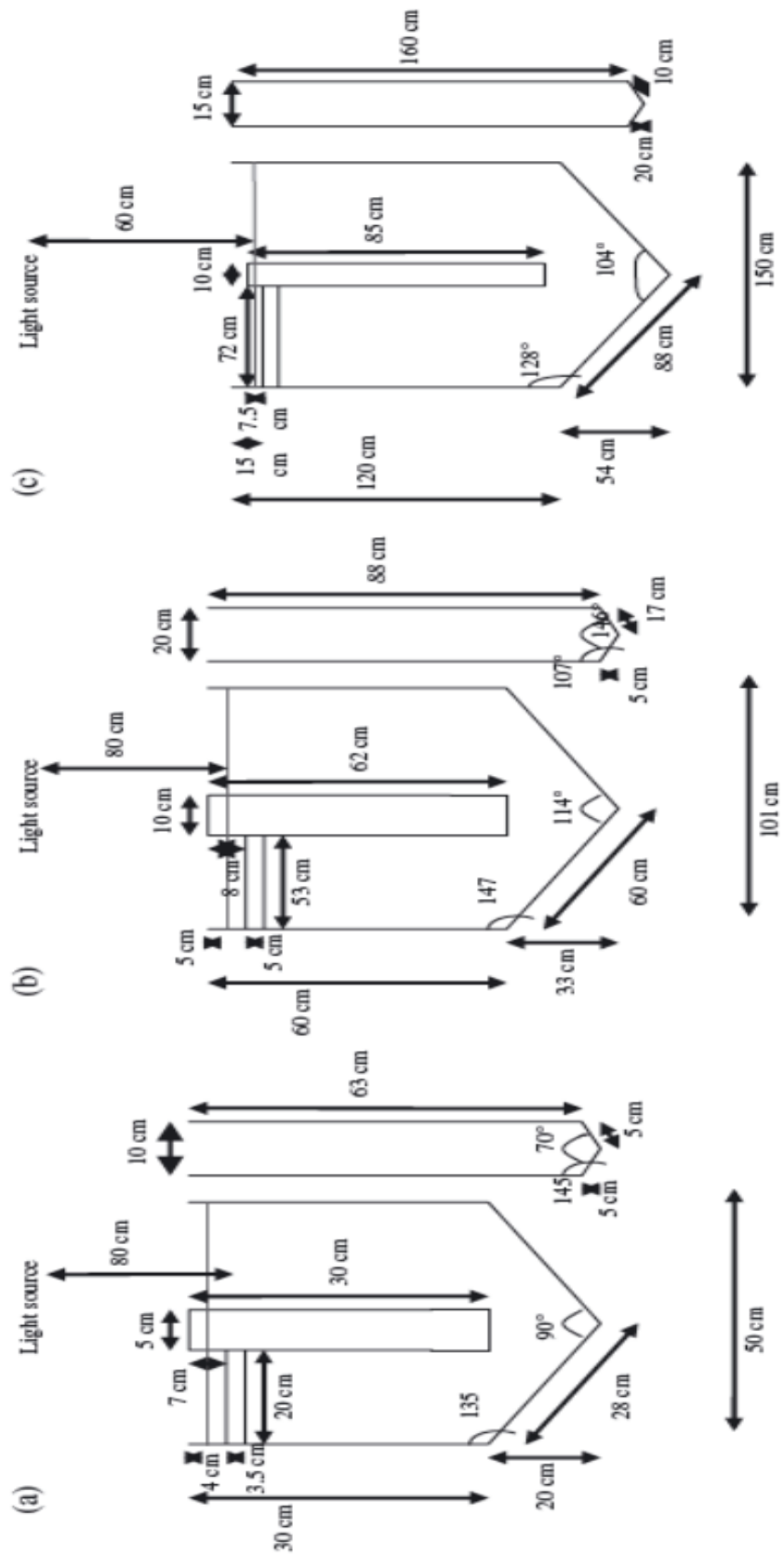


Figure 5 Tank drawings and dimensions of the three tanks of volumes (a)40, (b)500 and (c)2000 liters(Lika et al.,2015)

After all the dimensions and angles were used, one problem has occurred regarding the angles. Angles were not correct, hence they were changed and adjusted to fit the length of edges. After this, tank volume has increased to 545 liters. The geometry obtained in ANSYS Design Modeler is shown in figure 6.

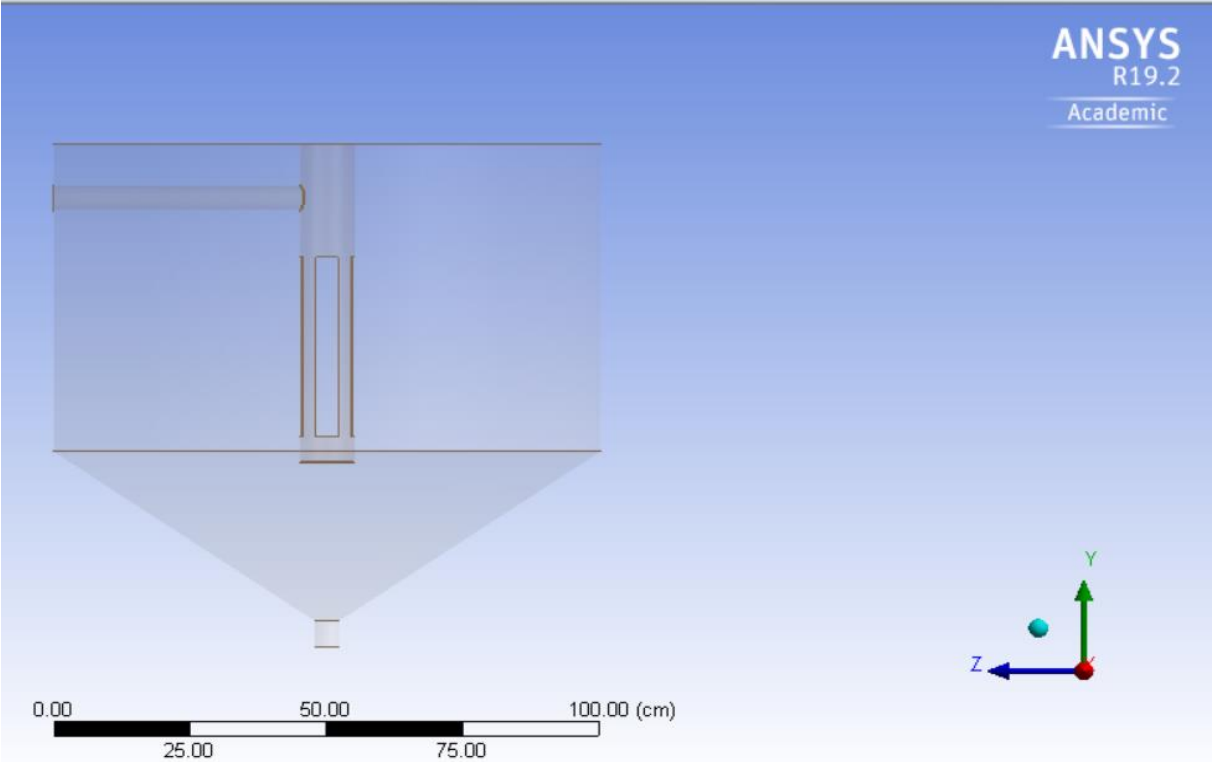


Figure 6 Obtained Geometry

After the process of designing geometry ended, the author has focused on the purpose which is to reach the best quality mesh for the model. Thus, three tetrahedral meshes were created, and they were prepared for the grid convergence index analysis. Three different element sizes and nodes were obtained by using a global element size option in ANSYS Meshing. Detailed information can be seen below in Table 1:

Global element size	Number of Elements	Nodes	Minimum Orthganal Quality	Max Skewness Quality	Max Aspect Ratio
50 mm	156800	30106	0.6799	0.93201	16.041
30 mm	284907	52954	0.6385	0.93614	18.428
23mm	487373	88343	0.6028	0.93796	23.82

Table 1 Quality of Meshes

When the results were assessed, it can be said that the mesh quality was good and proper for our purpose.

Good quality mesh means that mesh quality criteria are within the correct range: Low orthogonal quality or high skewness values are not recommended. Generally, it is important to try to keep minimum orthogonal quality >0.1 , or maximum skewness < 0.95 . However, these values may be different depending on the physics and the location of the cell. In addition that, the aspect ratio can be acceptable if the obtained value is in the range from 10 to 100. The bad quality mesh can cause convergence difficulties, bad physic description, diffuse solution. (ANSYS Training Material,2015)

In Figure 7 and Figure 8, the model which was obtained with 50 mm and 23 mm global size can be seen.

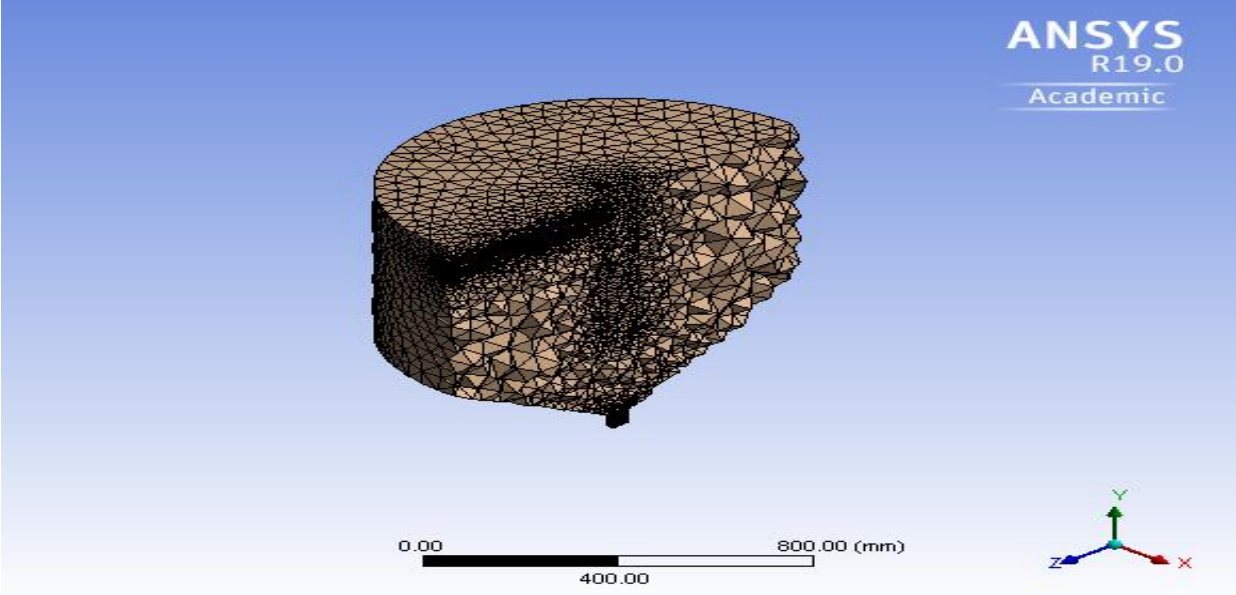


Figure 7 50 mm global size mesh

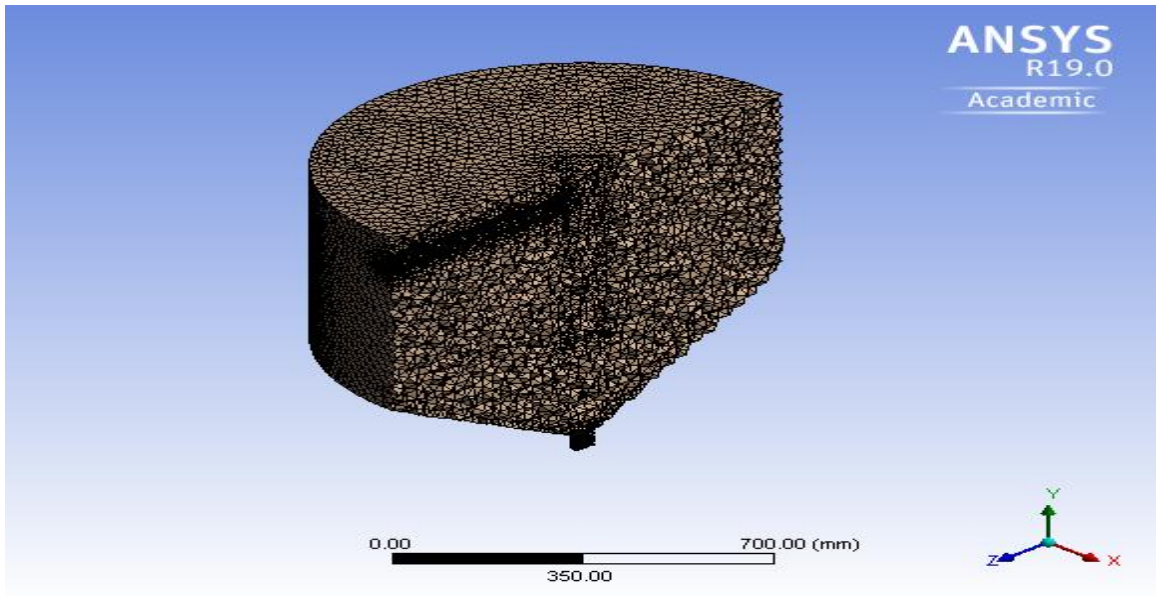


Figure 8 23 mm global size mesh

3.2. Grid Convergence Index

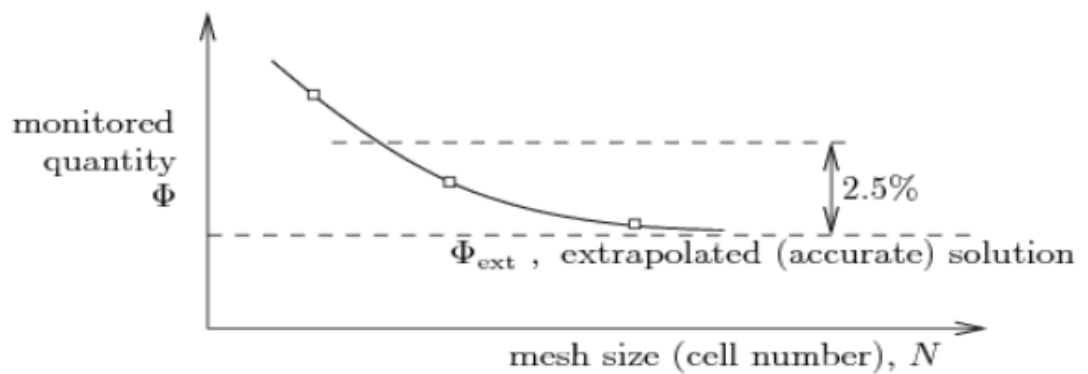


Figure 9 Monitored quantity to mesh size

The Grid Convergence Index (GCI) is used for determining the discretization error in a CFD simulation. It was calculated by using Matlab and a similar figure was obtained.

The dependence of the solution on the number of mesh (grid) cells (elements) can be described by the following equation:

$$\Phi = \Phi_{ext} + aN^{-p/D} \quad (15)$$

where Φ is the monitored quantity while Φ_{ext} is the extrapolated value and N represents the number of mesh elements, D is equal to 2 in 2-D case, and 3 in 3-D case. In our case, the monitored quantity was the average velocity in the given horizontal plane (the medium plane vertical distance is 30 cm from the top). The method involves performing the simulation three finer grids, p the order of the solution accuracy. (Peters, 2018)

$$\Phi_1 - \Phi_{ext} - aN^{-p/D1} = 0 \quad (16)$$

$$\Phi_2 - \Phi_{ext} - aN^{-p/D2} = 0 \quad (17)$$

$$\Phi_3 - \Phi_{ext} - aN^{-p/D3} = 0 \quad (18)$$

This value can be used to estimate the solution accuracy of individual mesh sizes result in percent

$$\varepsilon = \frac{\Phi_{ext} - \Phi_1}{\Phi_{ext}} \times 100 (\%) \quad (19)$$

The solution error and so called GCI index can be then expressed in percentage

$$\varepsilon_{21} = \frac{\Phi_1 - \Phi_2}{\Phi_1} \times 100 (\%) \quad (20)$$

$$GCI_{21} = \frac{1.25\varepsilon_{21}}{rp_{21} - 1} \quad (21)$$

$$r_{21} = \left(\frac{N1}{N2}\right)^{1/D} \quad (22)$$

Where 1.25 is a safety factor for calculation, and r_{21} is the rate ratio of the element size.

According to Celik (1993), the parameter p can be calculated as follows:

$$p = \frac{1}{\ln r_{21}} \left| \ln \left| \frac{\varepsilon_{32}}{\varepsilon_{21}} \right| + \ln \left(\frac{r_{21}^p - s}{r_{32}^p - s} \right) \right| \quad (23)$$

After the Matlab calculation, we have obtained the GCI (Grid Convergence Index) as 14% for the finest (largest) mesh, which could provide sufficient accuracy in many situations. Obtained graphic is shown in figure 10 and related Matlab script in Appendix A.

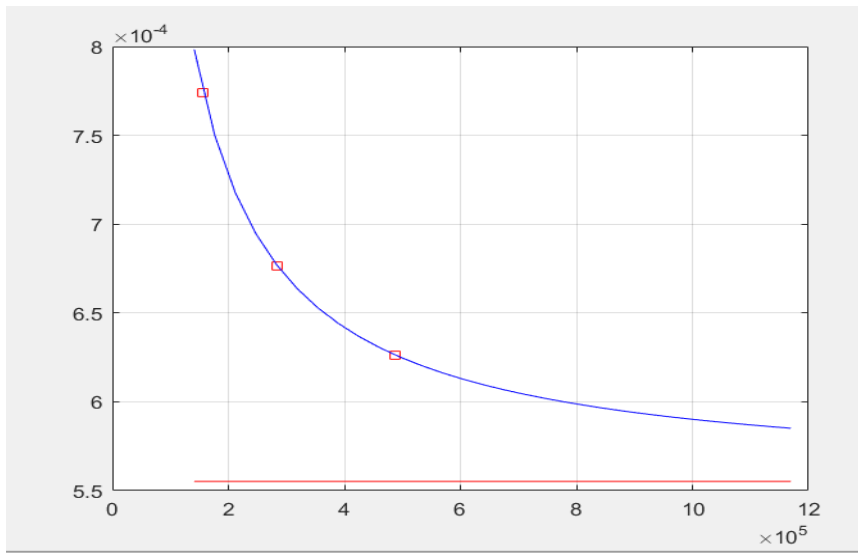


Figure 10 Average velocity vs size of the element

After this GCI, we can say our mesh quality is good and acceptable discretization error could occur in a CFD simulation. Once the GCI completed the main objective focused on choosing a turbulence model. For the better result number of elements increased to 845000. After that, GCI with Spalart Allmaras, $k-\varepsilon$ (with Realizable and enhanced wall treatment), $k-\omega$ (SST intermitting transitional) model was analyzed. According to GCI results (see table 2), the smallest error was found with the $k-\varepsilon$ model.

Turbulence model	GCI (%)
Spalart Allmaras	15.6985
$k-\varepsilon$ with Realizable+enhanced wall treatment	2.0265
$k-\omega$ SST intermitting transitional	10.2921

Table 2 GCI results in different turbulence model with 845000 mesh

3.3. Solver Settings

In the ANSYS Fluent solver, the symmetry boundary condition was used for the surface. Mesh quality was improved by changing the tetrahedral mesh elements into polyhedral. The number of elements was reduced to 258036, and the orthogonal quality increased to 0.89. The volumetric flow rate is 250 l/hr and inlet velocity is 0.35 m/s.

After that, the bottom, the medium, and the surface plane were created and different points were chosen in order to calculate velocity each point and take average velocities in these planes. Related points and velocities at each point are shown in table 4. When choosing these points, experiment data was used (Lika.K et al. 2015). After that, the thesis result was compared with the experimental result. Related planes are shown in figure 11.

Tank volume (l)	Layer	Velocity (cm s ⁻¹)
2000	Surface	$1.48 \times 10^{-2} \pm 1.32 \times 10^{-2}$
	Medium 1	$1.29 \times 10^{-2} \pm 1.04 \times 10^{-2}$
	Medium 2	$1.13 \times 10^{-2} \pm 9.36 \times 10^{-2}$
	Medium 3	$1.62 \times 10^{-2} \pm 4.57 \times 10^{-2}$
	Bottom	$6.61 \times 10^{-2} \pm 6.77 \times 10^{-2}$
500	Surface	$1.11 \times 10^{-2} \pm 1.19 \times 10^{-2}$
	Medium	$7.18 \times 10^{-3} \pm 7.91 \times 10^{-3}$
40	Bottom	$8.27 \times 10^{-3} \pm 1.12 \times 10^{-2}$
	Surface	$4.74 \times 10^{-3} \pm 9.45 \times 10^{-3}$
	Medium	$4.74 \times 10^{-3} \pm 4.96 \times 10^{-3}$
	Bottom	$4.80 \times 10^{-3} \pm 6.63 \times 10^{-3}$

Table 3 Experimental results with velocities at different planes with \pm values(Lika.K et al. 2015).

Surface Plane					
X	Y	Z	S_A	k_ε	k_ω_SST_INT
-45	10	0	8.45E-04	8.61E-04	1.42E-03
0	10	-45	8.53E-04	8.80E-04	1.53E-03
-25	10	0	1.59E-03	4.12E-04	9.28E-04
0	10	-25	1.68E-03	3.39E-04	1.12E-03
-10	10	0	1.73E-03	3.60E-03	1.30E-03
0	10	-10	1.69E-03	4.04E-03	1.17E-03
10	10	0	1.78E-03	3.15E-03	1.28E-03
0	10	10	1.78E-03	2.82E-03	1.04E-03
25	10	0	8.25E-04	2.25E-04	1.11E-03
0	10	25	6.94E-04	1.21E-04	9.69E-04
45	10	0	9.32E-04	7.63E-04	1.62E-03
0	10	45	8.58E-04	7.39E-04	1.33E-03
Medium Plane					
-45	25	0	1.15E-03	9.00E-04	1.51E-03
0	25	-45	1.20E-03	9.01E-04	1.80E-03
45	25	0	9.02E-04	8.25E-04	5.82E-04
0	25	45	2.73E-04	7.81E-04	1.08E-04
-25	30	0	6.95E-04	7.34E-04	1.01E-03
0	30	-25	6.60E-04	9.95E-04	6.74E-04
-10	30	0	7.78E-04	2.14E-03	8.72E-04
0	30	-10	7.44E-04	2.56E-03	6.12E-04
10	30	0	8.11E-04	1.70E-03	7.85E-04
0	30	10	5.84E-04	1.51E-03	3.24E-04
25	30	0	8.79E-04	4.46E-04	1.13E-03
0	30	25	6.19E-04	3.87E-04	4.64E-04
Bottom Plane					
-25	50	0	4.48E-04	5.33E-04	5.27E-04
0	50	-25	4.92E-04	6.45E-04	7.81E-04
25	50	0	4.66E-04	3.89E-04	6.38E-04
0	50	25	2.79E-02	3.26E-02	2.71E-02
-10	55	0	4.12E-04	1.06E-03	7.11E-04
0	55	-10	3.00E-04	1.17E-03	3.67E-04
10	55	0	6.59E-04	7.28E-04	8.77E-04
0	55	10	2.49E-04	1.67E-04	1.05E-04

Table 4 Velocities of each point

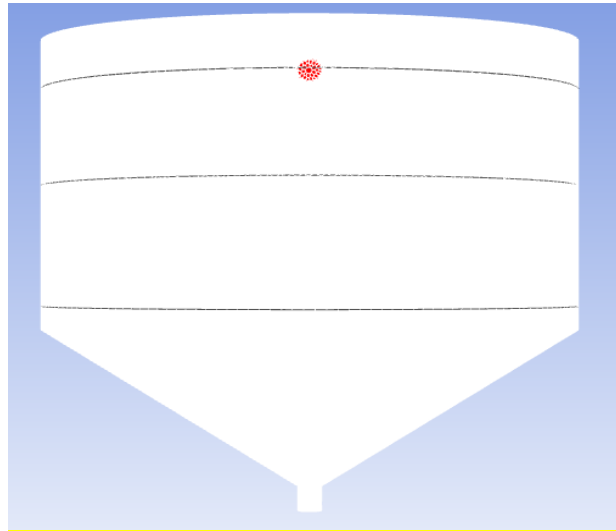


Figure 11 Bottom medium and surface planes in 545L tank.

Table 5 shows the experimental results of average velocities in different planes and their vertical distance from the surface.

experimental results	m/s	The vertical distance from the surface(m)
surface	1.11E-02	0.1
medium	7.18E-03	0.3
bottom	8.27E-03	0.55

Table 5 Experimental average velocities

Table 6 shows us calculated average velocities at different planes and different turbulence model. Moreover, it also shows us the differences between experimental velocity and the calculated velocity in the error section.

	surface(m/s)	Error (%)	medium(m/s)	Error (%)	bottom(m/s)	Error (%)
k-ε	1.50E-03	86.5205	1.16E-03	83.88948	4.66E-03	43.62831
k-w	1.24E-03	88.8647	8.22E-04	88.54784	3.89E-03	52.9086
S-A	1.27E-03	88.54626	7.75E-04	89.20473	3.87E-03	53.19617

Table 6 Calculated average velocities with errors

In this comparison, three simulations were performed in three different models. Firstly, we have started with the Spalart Allmaras Model and calculated velocities at each point in each plane and taken average velocities of them. In the surface plane, $1.27\text{E-}03$ m/s was found with 88.5% difference from the experimental result. In the medium plane, $7.75\text{E-}04$ m/s was assessed with 89.2% difference from the experimental result and in the bottom plane, $3.87\text{E-}03$ m/s which has 53.2% difference from experimental result.

After this, we have continued with the $k-\omega$ SST intermittency transitional model and average velocity was calculated in the surface plane as $1.24\text{E-}03$ m/s with 88.9% difference from the experimental result and in the medium plane $8.22\text{E-}04$ m/s was found with 88.5% difference from the experimental result and in the bottom plane $3.89\text{E-}03$ m/s was calculated with 52.9% difference from experimental result.

Finally, we have performed the simulation with the realizable $k-\varepsilon$ with enhanced wall treatment. In the surface plane $1.50\text{E-}03$ m/s was calculated with 86.5% difference from the experimental result and in the medium plane it was found as $1.16\text{E-}03$ m/s with 83.9% difference from the experimental result and in the bottom plane was calculated as $4.66\text{E-}03$ m/s with 43.6% difference from experimental result.

As it is seen in the above comparison, the minimum error was found for the realizable $k-\varepsilon$ model with enhanced wall treatment. To decide which is the best CFD model for fish tanks, the next step focused on comparing their symmetry with different models.

3.4. Symmetry

At first, we have compared the average velocities and checked the velocity profiles in the turbulence models. Generally, similar velocities are expected in each symmetric point when using the symmetric boundary conditions.

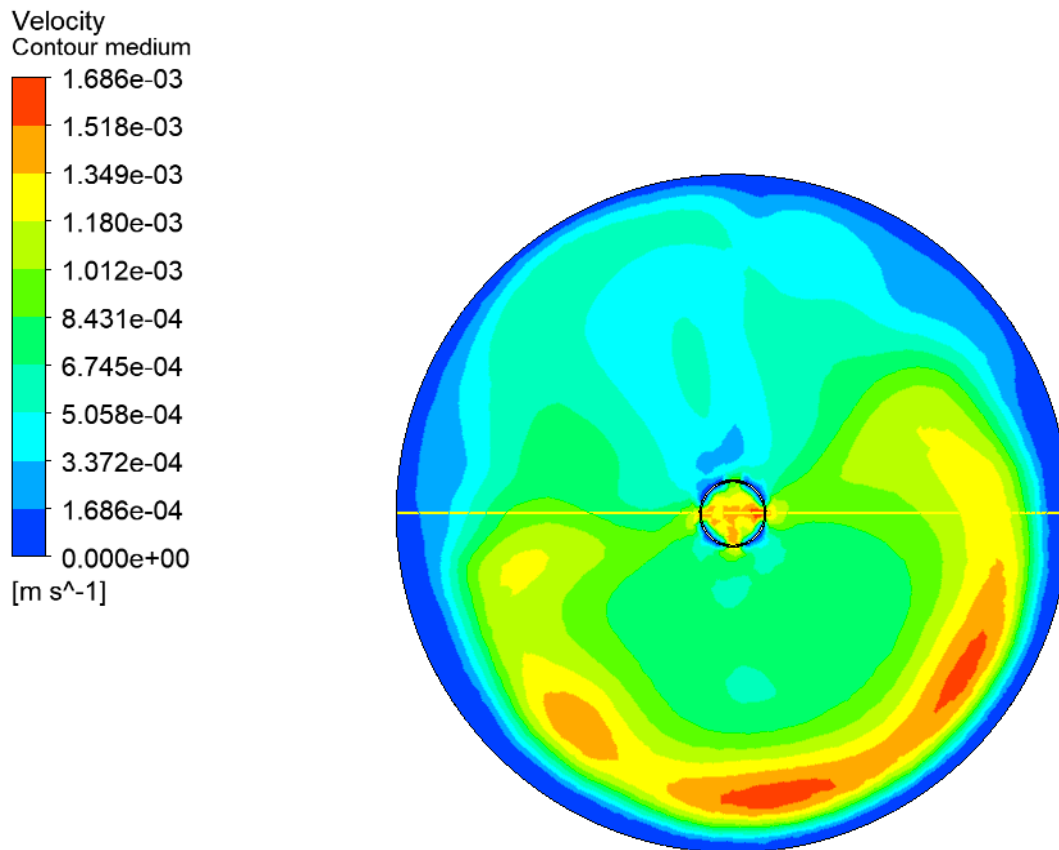


Figure 12 The $k-\omega$ SST intermitting transitional model

Figure 12 shows the $k-\omega$ model in the medium plane. According to this figure, the asymmetric profile can be seen clearly.

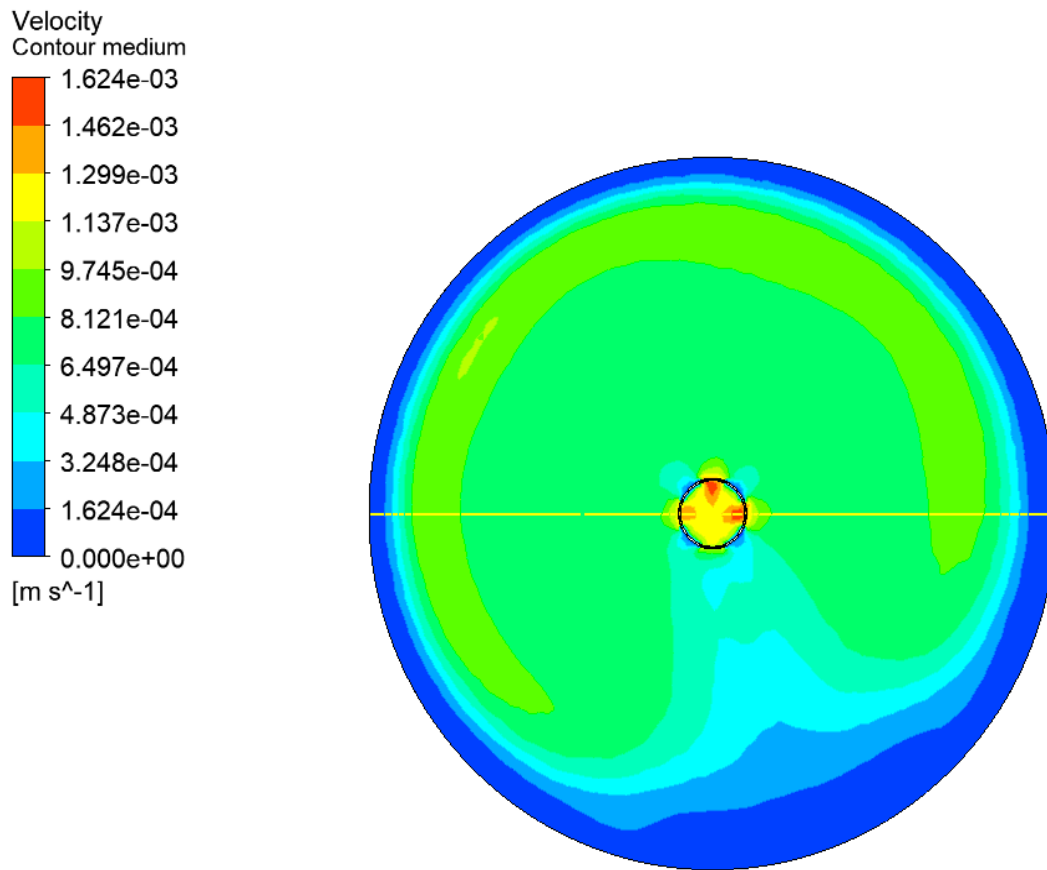


Figure 13 The Spalart Allmaras model

Figure 13 shows the velocity profile of the Spalart Allmaras model in the medium plane. In this figure, the asymmetric velocity profile is clearly visible.

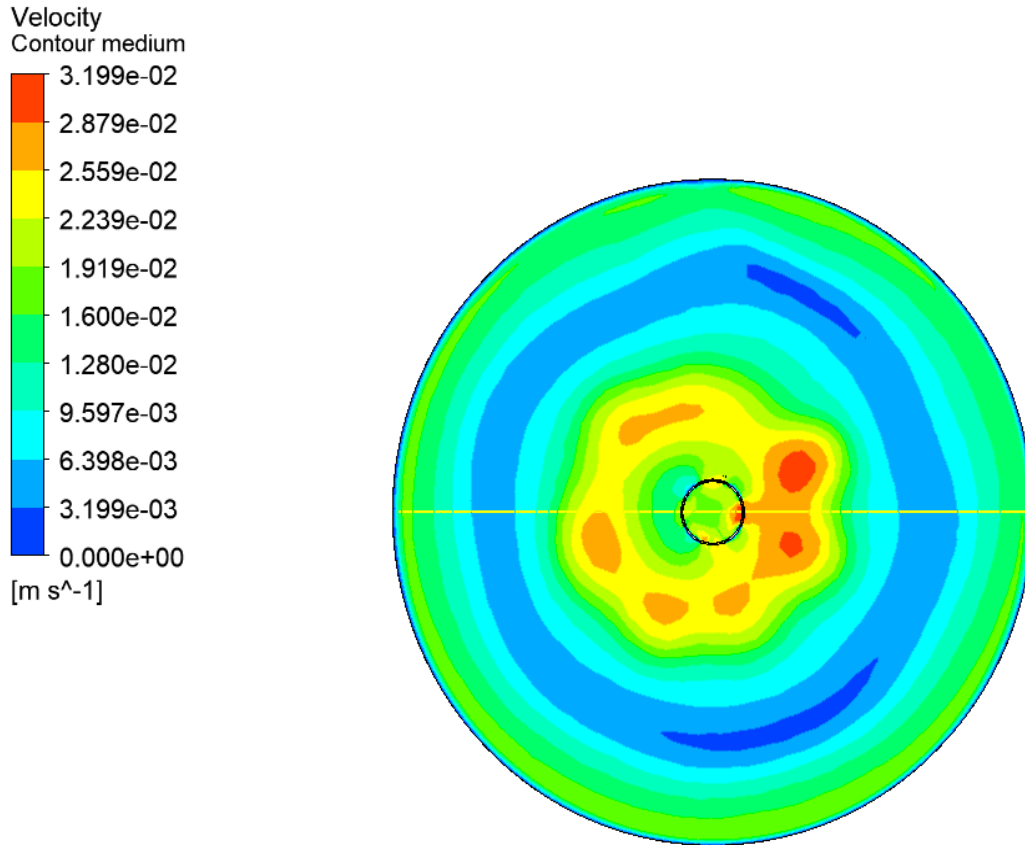


Figure 14 Realizable k- ε with enhanced wall treatment

Figure 14 represents to realizable k- ε model, and in this model our result is the most symmetric, therefore all simulations were then performed with this model

3.5. Bigger and Smaller Size Geometry Description

Once the most suitable turbulence model was found for the fish tanks, we have followed a comparison for different sizes of the fish tank. However, the problem is that the dimensions depicted in the article (Lika et al., 2015) are a little confusing and maybe not fully correct. Hence, to avoid problems when making bigger and smaller geometries, just the scale tool in the

Fluent solver was used. The scale factor for the bigger vessel was derived as $\left(\frac{2000}{500}\right)^{\frac{1}{3}} = 1.5874$, and for scaling down, it should be $\left(\frac{40}{500}\right)^{\frac{1}{3}} = 0.43$.

After applying these scale factors, we have obtained 45 liters and 2260 liters tanks. Then, in several created planes, different parameters were compared in terms of average velocity, maximum velocities, turbulent intensity, and uniformity index.

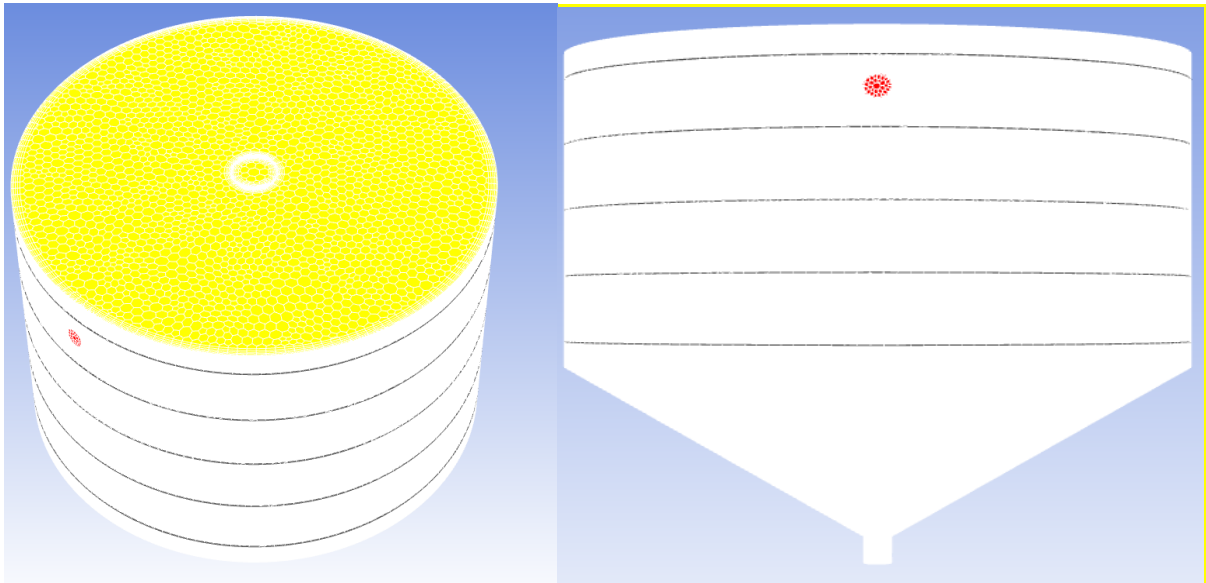


Figure 15 Created planes view after scaling

Figure 15 shows the created planes. Their distance can be seen in table 7. When creating these planes, we avoided the vertical location corresponding to the outlet pipe. The outlet pipe diameter is relatively small, giving large velocities which would substantially affect the average and maximum velocities. And because the fish is not present in this outlet pipe, it does not have any real impact on them.

Created Planes	The vertical distance from the liquid surface(m)
Surface	0.05
Medium-surface	0.175
Medium	0.3
Medium-bottom	0.375
Bottom	0.55

Table 7 Vertical distances of planes in figure 15

4. Results

“Realizable k- ϵ with enhanced wall treatment” model was used in the CFD simulations. Three different geometry were used and compared in order to find one correlation between each other and provide a source to biologists who want to choose fish tanks with corresponding volumes, and operational parameters.

Once obtained big and small size vessel, the uniformity index, turbulence intensity, average and maximum velocities were be calculated for different flow rates.

In general, one could assume that fish, and especially small fish(larvae), do not like large big non-uniformities in the velocity field. To evaluate these non-uniformities, ANSYS Fluent provides the uniformity index defined as follows (Papacek et al., 2018)

$$\gamma_a = 1 - \frac{\sum_i |u_i - u_{avg}| A_i}{2|u_{avg}| \sum_i A_i} \quad (24)$$

γ_a represents the variability of the velocity over the surface, when the value $\gamma_a = 1$ means the highest uniformity. u_{avg} represents the area-weighted average of the velocity. (Papacek et al., 2018)

$$u_{avg} = \frac{\sum_i u_i A_i}{\sum_i A_i} \quad (25)$$

Moreover, the turbulence intensity, also called as turbulence level, could be used to evaluate the impact of turbulent fluctuations on the fish.

$$I = \frac{u'}{U} \quad (26)$$

u' is the root mean square of the turbulent velocity fluctuations and U represents to the mean velocity

u' can find if there is turbulent energy(k) as follows:

$$u' = \sqrt{\frac{1}{3}(u'_x{}^2 + u'_y{}^2 + u'_z{}^2)} = \sqrt{\frac{2}{3}k} \quad (27)$$

U can be calculated with the three mean velocity components:

$$U = \sqrt{U_x^2 + U_y^2 + U_z^2} \quad (28)$$

Summary of the average and maximum velocities turbulence intensities and uniformity indices over the planes depicted in figure 15 for three different tanks and different flow rates are presented in the following table.

45 dm3				
\dot{V}/V	u-average	u-max	turbulent intensity	uniformity index
8.85E-02	1.25E-06	2.55E-04	7.40E-07	5.62E-01
1.77E-01	2.29E-06	4.65E-04	7.94E-07	7.11E-01
2.65E-01	4.17E-06	7.14E-04	4.58E-06	7.16E-01
3.54E-01	9.60E-06	9.57E-04	1.89E-05	7.10E-01
4.42E-01	1.81E-05	1.16E-03	3.77E-05	6.97E-01
5.31E-01	3.25E-05	1.39E-03	6.18E-05	6.79E-01
6.19E-01	4.68E-05	1.58E-03	7.81E-05	6.62E-01
7.08E-01	6.44E-05	1.80E-03	9.48E-05	6.48E-01
7.96E-01	8.10E-05	2.02E-03	1.10E-04	6.40E-01
1.00E+00	1.12E-04	2.48E-03	1.40E-04	6.42E-01
565 dm3				
\dot{V}/V	u-average	u-max	turbulent intensity	uniformity index
8.85E-02	7.99E-05	2.53E-03	1.69E-04	6.74E-01
1.77E-01	1.31E-04	4.87E-03	2.89E-04	6.44E-01
2.65E-01	2.77E-04	7.12E-03	4.69E-04	6.91E-01
3.54E-01	5.13E-04	9.36E-03	6.51E-04	7.27E-01
4.42E-01	8.56E-04	1.16E-02	7.89E-04	7.52E-01
5.31E-01	1.15E-03	1.37E-02	8.90E-04	7.45E-01
6.19E-01	1.43E-03	1.62E-02	9.98E-04	7.34E-01
7.08E-01	1.66E-03	1.84E-02	1.09E-03	7.25E-01
7.96E-01	1.88E-03	2.05E-02	1.19E-03	7.20E-01
1.00E+00	2.35E-03	2.53E-02	1.39E-03	7.15E-01
2260 dm3				
\dot{V}/V	u-average	u-max	turbulent intensity	uniformity index
8.85E-02	7.35E-04	9.15E-03	6.32E-04	7.47E-01
1.77E-01	1.64E-03	1.79E-02	9.68E-04	7.11E-01
2.65E-01	2.49E-03	2.63E-02	1.34E-03	7.13E-01
3.54E-01	3.46E-03	3.46E-02	1.69E-03	7.21E-01
4.42E-01	4.58E-03	4.28E-02	2.10E-03	7.31E-01
5.31E-01	5.65E-03	5.16E-02	2.49E-03	7.33E-01
6.19E-01	6.74E-03	5.92E-02	2.88E-03	7.37E-01
7.08E-01	7.78E-03	6.68E-02	3.21E-03	7.38E-01
7.96E-01	8.88E-03	7.58E-02	3.54E-03	7.37E-01
1.00E+00	1.13E-02	9.45E-02	4.35E-03	7.42E-01

Table 8 Calculated turbulent intensity, uniformity index, average, and maximum velocity

According to these data, the aim was to find only one correlation for three sizes of the tanks which would describe the given quantity.

For example, the averaged velocities for all three tank sizes could be described by a single correlation like;

$$u_{avg} = f\left(\frac{\dot{V}}{V}, \dots\right) \tag{29}$$

The average velocity, which was evaluated over several planes in the fish tank looks like the following for the three tank sizes.

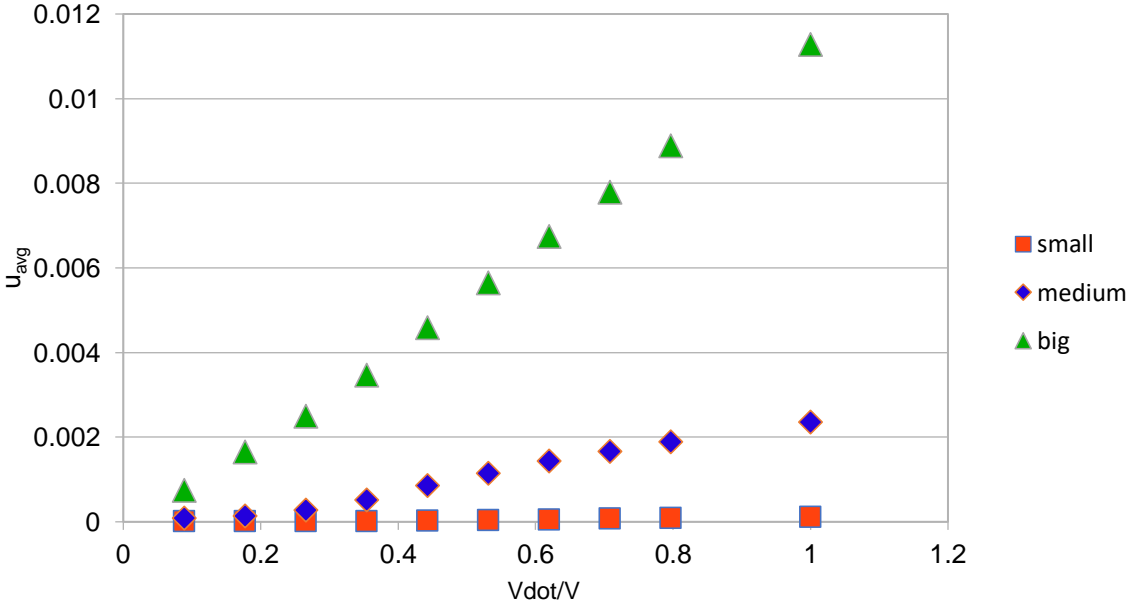


Figure 16 u_{avg} vs \dot{V}/V

According to figure 16, it cannot be clearly said there is such a correlation. It is probably better to use some dimensionless velocity instead of the absolute velocity u_{avg}

$$u_{avg}^* = u_{avg}/u_{ref} \tag{30}$$

where we could use the inlet velocity as the reference velocity which is the most obvious approach. The dependency is shown in figure 17:

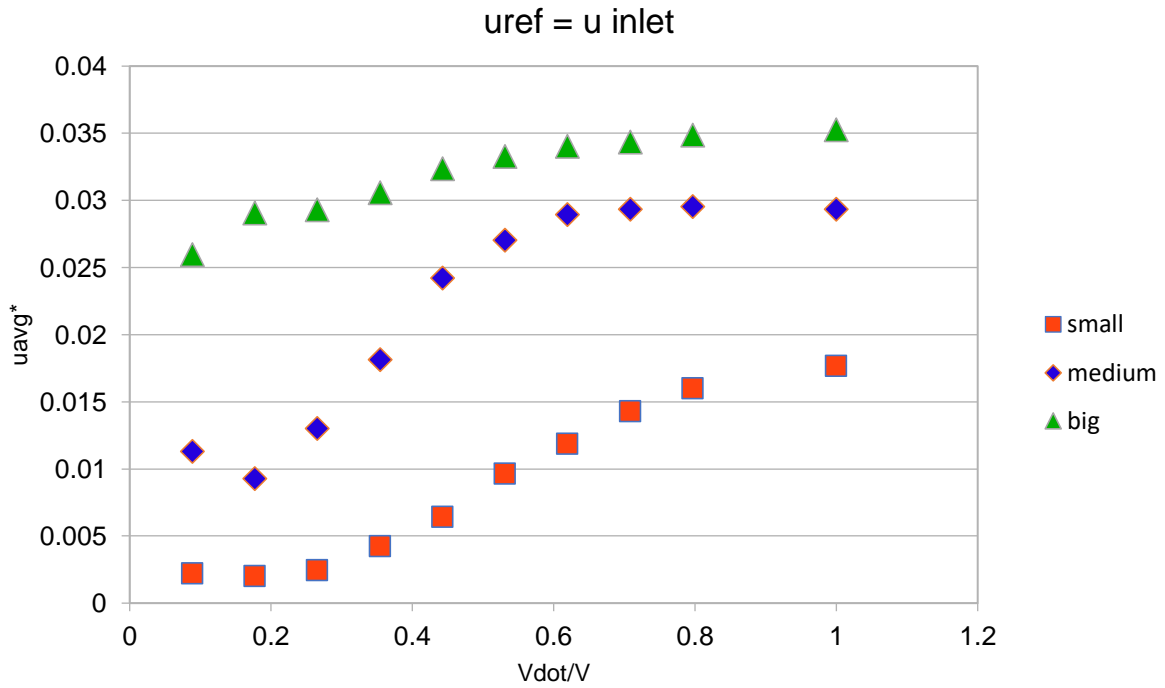


Figure 17 u_{avg}^* vs \dot{V}/V

There is still a clear difference between the different sizes of tanks (see small, medium and big in the legend of figure 17). In order to get it more close together, we have tried to use the maximum of the averaged velocities for particular tank sizes as the reference velocity u_{ref} .

$$u_{ref} = \max(u_{avg}) \quad (31)$$

The dependency of this value with respect to the tank volume is shown in figure 18.

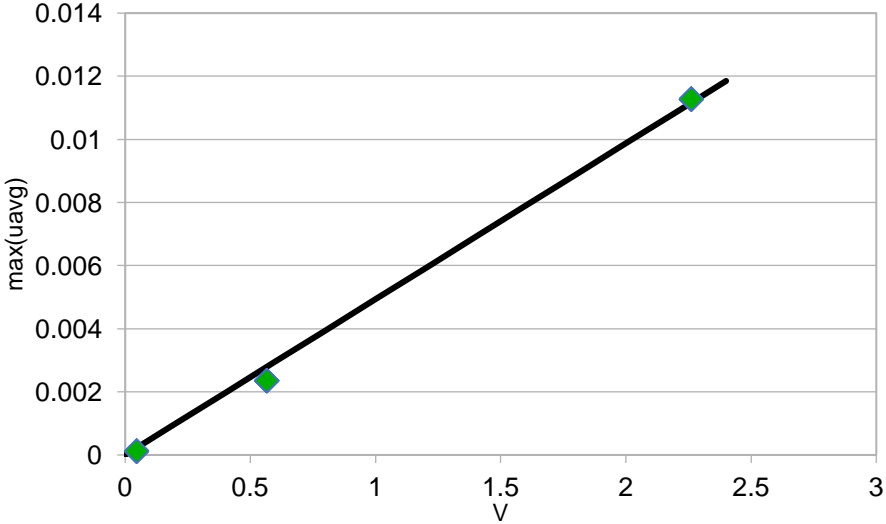


Figure 18 Max(u_{avg}) vs Volume

According to figure 18, it can be described as a linear function:

$$u_{ref} = c_1 V \tag{32}$$

This definition of u_{ref} transforms the dependency of the dimensionless velocity u_{avg}^* represented by the following figure

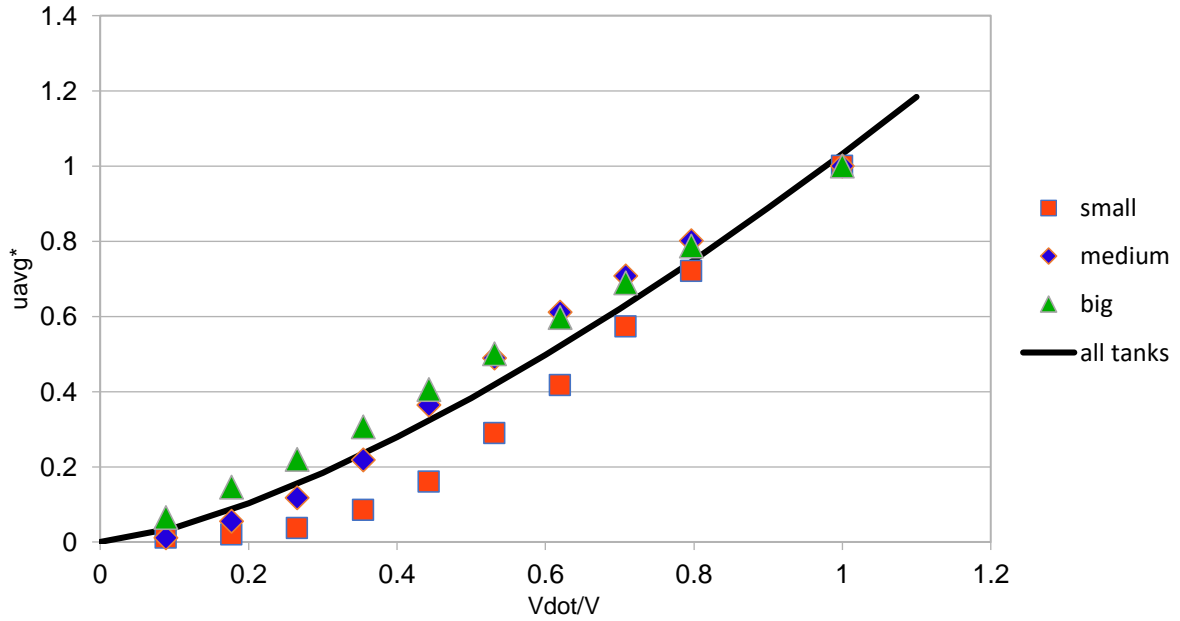


Figure 19 $u_{ref} = \max(u_{avg})$

Here, the data for different tank sizes are more close together, and they can be described by the following function.

$$u_{avg}^* = c_2 \left(\frac{\dot{V}}{V} \right)^m \quad (33)$$

Using the definition of the reference value above (Equation 32) one can describe the absolute average velocity for some tank of a given size as

$$u_{avg} = c_{12} \left(\frac{\dot{V}}{V} \right)^m V \quad (34)$$

where $c_{12} = c_1 c_2$ for the turbulence intensity calculated parameters c_1 , c_2 and m , including their confidence intervals provided in table 9

Vdot/V	u_{avg}^*			V	max(uavg) vs V		
0	0	c2	confidence intervals	0	0	c1	Confidence intervals.
0.1	0.03827681	1.032844	7.52%	0.2	0.0009876	0.004938	12.46%
0.2	0.1032142	m		0.4	0.0019752		
0.3	0.1843926	1.431099	13.44%	0.6	0.0029628		
0.4	0.27831921			0.8	0.0039504		
0.5	0.38302843			1	0.004938		
0.6	0.49721842			1.2	0.0059256		
0.7	0.61994718			1.4	0.0069132		
0.8	0.75049345			1.6	0.0079008		
0.9	0.88828276			1.8	0.0088884		
1	1.032844			2	0.009876		
1.1	1.18378208			2.2	0.0108636		
				2.4	0.0118512		

Table 9 Corresponding values for average velocity

It can be assessed that it is not perfect for the average velocities and three tank sizes. On the other hand, for maximum velocities the data for all three tank sizes are perfectly aligned which can be seen in the next figure:

There, the reference velocity is given as

$$u_{ref} = \max(u_{max}) = c_1 V \quad (35)$$

And dimensionless maximum velocity can be then described similarly as for the average velocity.

$$u_{max}^* = c_2 \left(\frac{\dot{V}}{\bar{V}} \right)^m \quad (36)$$

$$u_{max} = c_{12} \left(\frac{\dot{V}}{\bar{V}} \right)^m V \quad (37)$$

where $c_{12} = c_1 c_2$ for the turbulence intensity calculated parameters c_1 , c_2 and m , including their confidence intervals provided in table 10

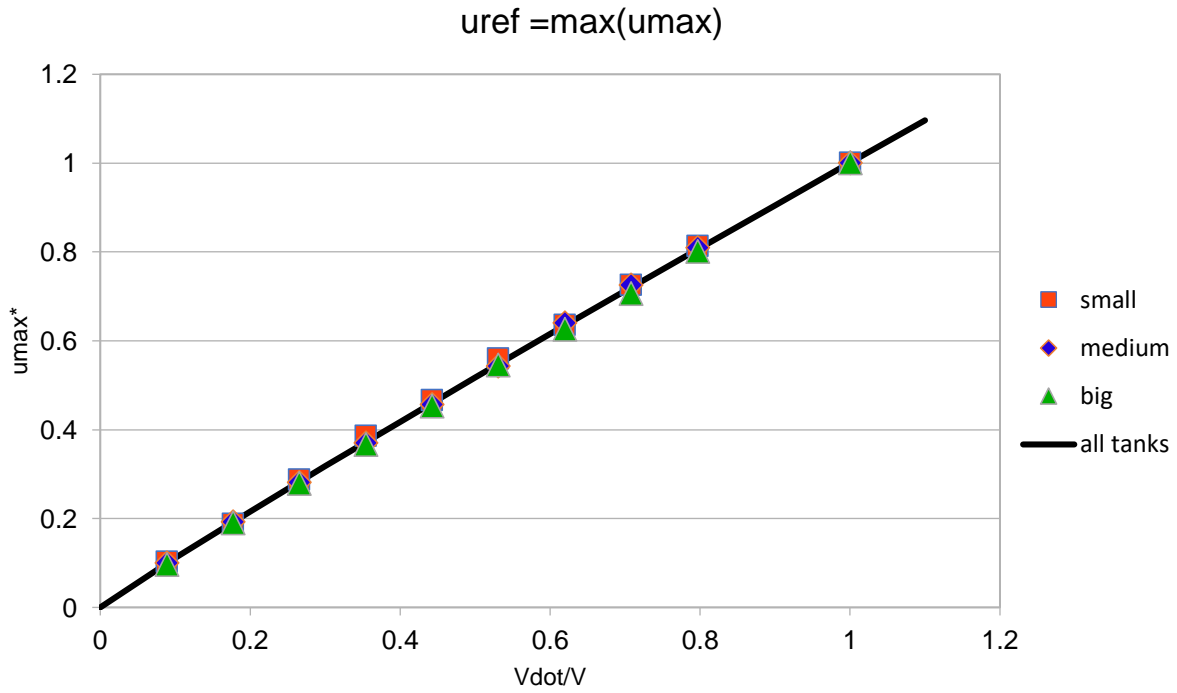


Figure 20 u_{max}^* vs \dot{V}/V

\dot{V}/V	u_{max}^*			V	max(u_{max}) vs V		
0	0	c2	confidence intervals	0	0	c1	confidence intervals
0.1	0.11155294	1.001182	0.54%	0.2	0.0084002	0.042001	5.38%
0.2	0.21595947	m		0.4	0.0168004		
0.3	0.31782851	0.953032	1.10%	0.6	0.0252006		
0.4	0.41808393			0.8	0.0336008		
0.5	0.51715629			1	0.042001		
0.6	0.61529598			1.2	0.0504012		
0.7	0.71266677			1.4	0.0588014		
0.8	0.80938414			1.6	0.0672016		
0.9	0.90553383			1.8	0.0756018		
1	1.001182			2	0.084002		
1.1	1.09638122			2.2	0.0924022		
				2.4	0.1008024		

Table 10 Corresponding values of u_{max}^*

Figure 21 shows us a comparison of turbulence intensity with \dot{V}/V . There is still a difference between the different sizes of tanks which can be seen in figure 21. However, we have aligned points of three sizes of tanks, especially in the bigger flow rates.

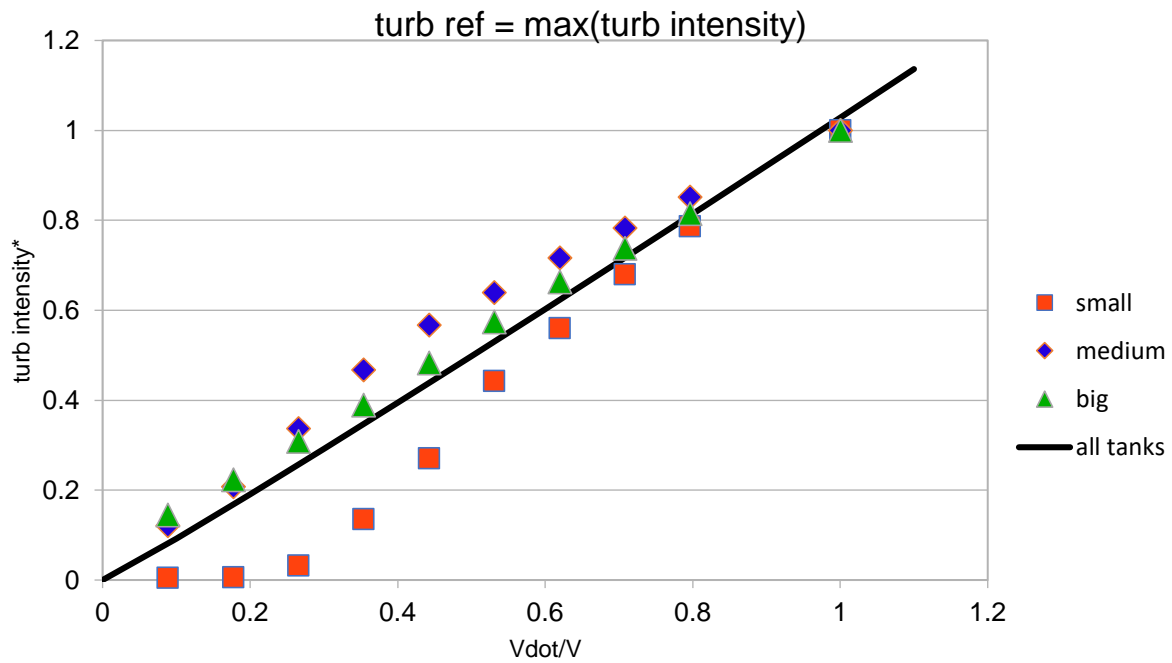


Figure 21 Turbulence Intensity vs \dot{V}/V

$$turb_{max}^* = c_2 \left(\frac{\dot{V}}{V} \right)^m \quad (38)$$

$$turb_{max} = c_{12} \left(\frac{\dot{V}}{V} \right)^m V \quad (39)$$

where $c_{12} = c_1 c_2$ for the turbulence intensity calculated parameters c_1 , c_2 and m , including their confidence intervals provided in table 11

Vdot/V	turbulence*			V	max(turb) vs V		
0	0	c2	confidence intervals	0	0	c1	confidence intervals
0.1	0.09241542	1.028453	8.64%	0.2	0.000391	0.001955	20.05%
0.2	0.1908773	m		0.4	0.000782		
0.3	0.2917583	1.04644	16.86%	0.6	0.001173		
0.4	0.39424311			0.8	0.001564		
0.5	0.49793725			1	0.001955		
0.6	0.60260543			1.2	0.002346		
0.7	0.70809062			1.4	0.002737		
0.8	0.81428031			1.6	0.003128		
0.9	0.92108982			1.8	0.003519		
1	1.028453			2	0.00391		
1.1	1.13631676			2.2	0.004301		
				2.4	0.004692		

Table 11 Corresponding values of $turb_{max}^*$

For the uniformity index, there is no clear dependency between the three tanks. In general, we can say that the bigger is the flow rate, the better (higher) is the uniformity index. Figure 22 shows us the distribution of different sized tanks. Table 12 shows us ANSYS results for uniformity index. According to these results, a higher flow rate is better, but it might be limiting for the fish inside the tank.

Vdot/V	Uniformity Index		
	45 L	565 L	2260 L
8.85E-02	5.62E-01	6.74E-01	7.47E-01
1.77E-01	7.11E-01	6.44E-01	7.11E-01
2.65E-01	7.16E-01	6.91E-01	7.13E-01
3.54E-01	7.10E-01	7.27E-01	7.21E-01
4.42E-01	6.97E-01	7.52E-01	7.31E-01
5.31E-01	6.79E-01	7.45E-01	7.33E-01
6.19E-01	6.62E-01	7.34E-01	7.37E-01
7.08E-01	6.48E-01	7.25E-01	7.38E-01
7.96E-01	6.40E-01	7.20E-01	7.37E-01
1.00E+00	6.42E-01	7.15E-01	7.42E-01

Table 12 Uniformity index for three sizes of tanks

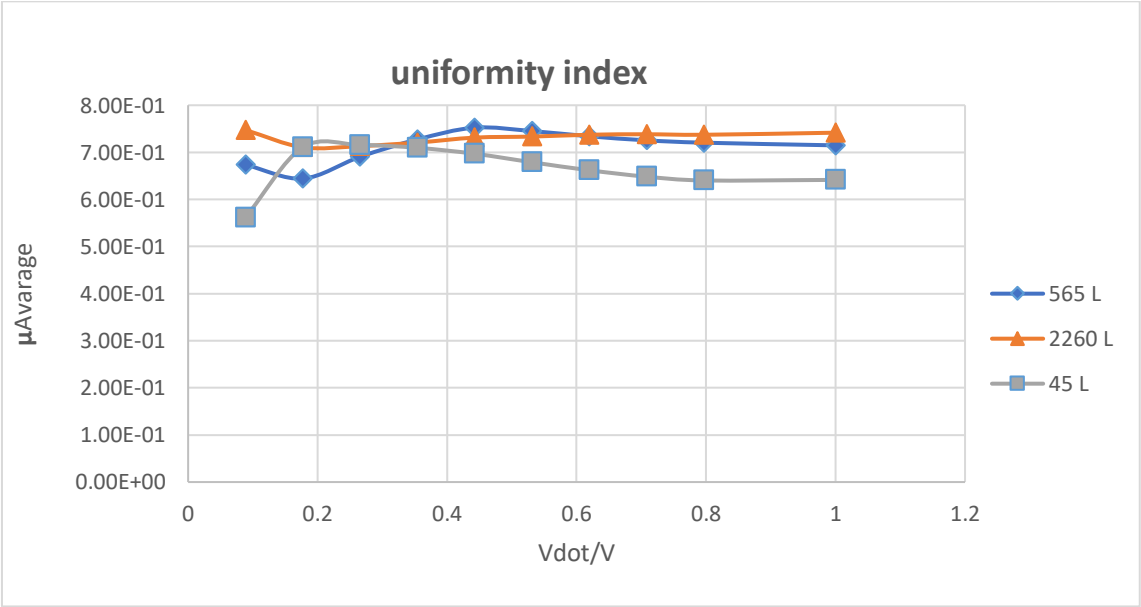


Figure 22 Uniformity Index of three sizes of tanks

5. Conclusion

The purpose of this paper was to find the best CFD model for fish tanks and their operating parameters. Generally, it focused on how to choose operating parameters and provide good living conditions in fish tanks.

3-D geometry for the fish tank was created in ANSYS DesignModeler. It was a cylindrical tank with a conical bottom described by Lika et al. (2015). Then, ANSYS Meshing was used to create a tetrahedral mesh. Firstly, the simulations were performed using the Spalart-Allmaras turbulent model. After that, the grid convergence index was analyzed and compared with $k-\epsilon$ and $k-\omega$ turbulent models. According to comparisons, the smallest discretization error was found in the $k-\epsilon$ model.

According to (Lika et al., 2015) experimental data, boundary conditions were created in ANSYS Fluent solver which was used to get results. After that, average velocities were calculated with Spalart-Allmaras, $k-\omega$ and $k-\epsilon$ turbulent model and they were compared with the experimental data to find the most suitable model. Finally, symmetry of results was analyzed. The results have shown that the $k-\epsilon$ model is the most suitable model for the fish tanks in our case, and has a better distribution of the velocity in tanks.

Once we have selected the turbulence model, geometries of three different sizes were created in order to find relations of some quantities on operational parameters. To create bigger and smaller geometries, scaling factor was used because in the article (Lika et al., 2015) some discrepancies in the geometry description were found. Tetrahedral mesh was transformed to polyhedral so that the mesh quality improved and better convergence of the solution could be obtained. After that, we have evaluated turbulence intensity, uniformity index, average velocities, and maximum velocities (the results can be seen in Table 8) in several horizontal planes of the tanks.

According to these results, one correlation describing corresponding quantity (average velocity, maximum velocity, and turbulence intensity) in all three tanks was evaluated so that it could provide an important source of information to biologists who want to choose a fish tank with corresponding volume and operational parameters.

Although there was identified no correlation for the uniformity index between the three tanks, but generally we can say that higher flow rates provide a better (higher) uniformity index. One

must of course take into account that there might exist limiting values for velocities or turbulence intensities from the biological point of view.

For further improvements:

- Using some food particles and performed new simulations to validate the CFD results and investigate self-cleaning capabilities.
- Using different size geometries and trying to find a new correlation between each other.

REFERENCES

Aerospace, Mechanical & Mechatronic Eng. University of Sydney (2005), Classification Of Flows, Laminar And Turbulent Flows, http://www-mdp.eng.cam.ac.uk/web/library/enginfo/aerothermal_dvd_only/aero/fprops/pipeflow/node8.html

ANSYS Training Material,2014

Bhaskaran R., Collins L. (2012), Introduction to CFD Basics. available online at <http://dragon-fly.tam.cornell.edu/teaching/mae5230-cfd-intro-notes.pdf>

Hinze J. O., (1975)Turbulence, McGraw-Hill

Hu H. H.(2012), Fluid Mechanics (Fifth Edition), Computational Fluid Dynamics, Pages 421-472, available online at <https://www.sciencedirect.com/science/article/pii/B9780123821003100101>

Lika K., Pavlidis M., Mitrizakis N., Samaras A. and Papandroulakis N. (2015) The Fisheries Society of the British Isles, Journal of Fish Biology 86, 1271–1285 doi:10.1111/jfb.12636, available online at wileyonlinelibrary.com

Moukalled F., Mangani L. a Darwish M.(2015), The Finite Volume Method in Computational Fluid Dynamics: An Advanced Introduction with OpenFOAM® and Matlab®. ISBN 978-3-319-16873-9.

Papacek S., Petera K., Masalo I. and Oca J.(2018), On the optimization of recirculated aquaculture systems.

Petera K., (2018) (Lecture notes CFD,(2018)]

Souza M. (2018), The Benefits of Aquaculture, available online at <https://www.thebalance.com/the-benefits-of-aquaculture-1301626>

Wilcox C., David(2006) Turbulence Modeling for CFD. Third Edition.

Zuo W.(2005), introduction Of Computational Fluid Dynamics, available online at http://www-mayr.informatik.tu-muenchen.de/konferenzen/Jass05/courses/2/Zuo/Zuo_paper.pdf

Appendix A

```
N = [ 156800 284910 487370 ];
```

```
Phi = [ 0.00077429661 0.00067646386 0.00062644786 ];
```

```
[N, i] = sort(N,'descend'); % reverse order of elements so that the first element represent the finest mesh
```

```
Phi = Phi(i);
```

```
figure(1);
```

```
plot(N,Phi,'r*', N,Phi,'b');
```

```
grid on;
```

```
D = 3; % dimension of the problem, 2-D or 3-D
```

```
r21 = (N(1)/N(2))^(1/D)
```

```
r32 = (N(2)/N(3))^(1/D)
```

```
if ( r21 < 1.3 || r32 < 1.3 )
```

```
    disp('refinement factors r21 and r32 should be greater than 1.3');
```

```
end
```

```
eps32 = Phi(3)-Phi(2)
```

```
eps21 = Phi(2)-Phi(1)
```

```
R = eps21/eps32
```

```
s = sign(eps32/eps21)
```

```
fq = @(p) log((r21.^p-s)./(r32.^p-s));
```

```
fp = @(p) p - 1/log(r21)*abs(log(abs(eps32/eps21))+fq(p));
```

```
%p = fzero(fp,1)
```

```
p = fsolve(fp,1)
```

```
Phi21ext = (r21^p*Phi(1)-Phi(2))/(r21^p-1)
```

```
e21a = abs((Phi(1)-Phi(2))/Phi(1))*100
```

```

CGI21 = 1.25*e21a/(r21^p-1)

e32a = abs((Phi(2)-Phi(3))/Phi(2))*100
CGI32 = 1.25*e32a/(r32^p-1)

CGI33 = 1.25*abs(Phi21ext-Phi(3))/Phi(3)*100
fun = @(x,N) x(1)+x(2)*N.^(-x(3)/D);

feqs = @(x) [ ...
    fun(x,N(1)) - Phi(1); ...
    fun(x,N(2)) - Phi(2); ...
    fun(x,N(3)) - Phi(3) ...
];

b = fsolve(feqs, [ Phi(1), 1, 1 ])

Phi_ext = b(1)
p = abs(b(3))
eps = abs(Phi_ext - Phi(1))/Phi_ext*100

e21a = abs((Phi(1)-Phi(2))/Phi(1))*100
e21ext = abs((Phi_ext-Phi(1))/Phi_ext)*100
GCI21 = 1.25*e21a/(r21^p-1)

figure(2);
plot(N,Phi,'rs');
hold on;
n = linspace(0.9*N(3),2.4*N(1),30);
plot(n,Phi_ext*ones(1,length(n)), 'r');
plot(n,fun(b,n), 'b');
text(200000,6.185, 'Phi ext');
hold off;
grid on;
h1 = 50; h2 = h1*r21; h3 = h2*r32;

```

```

h = [ h1 h2 h3 ]
fun2 = @(x,h) x(1)+x(2)*h.^x(3);
feqs2 = @(x) [ ...
    fun2(x,h(1)) - Phi(1); ...
    fun2(x,h(2)) - Phi(2); ...
    fun2(x,h(3)) - Phi(3) ...
];

b = fsolve(feqs2, [ Phi(1), 1, 1 ])
Phi_ext = b(1)
p = abs(b(3))
a = b(2)
hs = linspace(0,1.1*h3);
figure(3);
plot(h,Phi,'r*', hs,fun2(b,hs),'b',[0 hs(end)],[Phi_ext Phi_ext],'r');
hold on;
text(1.5,6.185,'Phi ext');
hold off;
grid on;

```